

Interfacial thermal conductance between silicon and a vertical carbon nanotube

Ming Hu,^{1,a)} Pawel Koblinski,^{1,2,a)} Jian-Sheng Wang,³ and Nachiket Raravikar⁴

¹*Rensselaer Nanotechnology Center, Rensselaer Polytechnic Institute, Troy, New York 12180, USA*

²*Department of Materials Science and Engineering, Rensselaer Polytechnic Institute, Troy, New York 12180, USA*

³*Center for Computational Science and Engineering and Department of Physics, National University of Singapore, Singapore 117542, Singapore*

⁴*Intel Corporation, 5000 W. Chandler Blvd., Chandler, Arizona 85226, USA*

(Received 30 July 2008; accepted 25 August 2008; published online 20 October 2008)

Molecular simulations are used to evaluate thermal resistance between crystalline silicon and a vertically oriented carbon nanotube (CNT). Without chemical bonds between CNT and Si the thermal resistance is high and its values are consistent with that measured in experiment on vertical CNT arrays. With chemical bonds the thermal resistance is reduced by two orders of magnitude demonstrating significant potential of CNT arrays for thermal management applications. The underlying mechanism for the very large effect of chemical bonding is revealed by simulations of individual phonon scattering across the interface and understood within an analytical solution of a simple spring-mass chain model. © 2008 American Institute of Physics. [DOI: 10.1063/1.3000441]

I. INTRODUCTION

Efficient heat dissipation is one of the crucial challenges that limit the development of disruptive microelectronic device technologies. The International Technology Roadmap for Semiconductors 2004 (Refs. 1 and 2) estimates suggest that an 8 nm feature-size device may generate local heat flux as high as $100\,000\text{ W/cm}^2$ that would need to be dissipated efficiently to preserve device integrity, reliability, and performance. The anticipated heat flux at the die level is $\sim 1000\text{ W/cm}^2$, which is ten-fold higher than present complementary metal oxide semiconductor devices,³ making power dissipation perhaps the most important factor that limits the device density on each chip. Although large air fans and/or liquid based cooling solutions have been applied and can dissipate more than 100 W of total power, thermal resistances at multiple interfaces from the die through the heat spreader to the outside heat sink remain a bottleneck.

Carbon nanotubes (CNTs), due to their very high intrinsic thermal conductivity,^{4,5} are considered for improvement of heat dissipation in microelectronic devices.^{6–12} Recently, Xu and Fisher^{6,7} fabricated and determined heat conduction of thermal interfaces that employ CNT arrays. In their work, the addition of the CNT array to phase change materials (PCM) reduced the overall resistance of the Cu-PCM-Si interface by a factor of 4. In the case of Cu–In–Si interface, the addition of the CNT array has a minor effect on the overall resistance.⁷ Tong *et al.*⁸ studied the thermal properties of a three-layer test configuration, which consisted of a CNT array grown on Si substrate directly and adhered to a glass plate. They measured the Si-CNT interfacial conductance to be about $10^6\text{ W/m}^2\text{ K}$. The glass-CNT interfaces with only physical bonding (van der Waals) has a thermal conductance

of about $10^5\text{ W/m}^2\text{ K}$. By bonding the nanotubes and glass using an indium weld, they observed an order of magnitude enhancement in the overall thermal conductance ($\sim 2.2 \times 10^6\text{ W/m}^2\text{ K}$). Recent modeling work by Diao *et al.*¹³ demonstrated that increased pressure between CNT and Si surface leads to increased thermal conductance due to increased nonbonded interactions and formation of chemical bonds.

The experiments clearly established the importance of interfacial bonding on thermal resistance. However, due to inherent difficulties in characterizing such bonding for large arrays of CNTs, it is not obvious what are the upper limits on the interfacial conductance and what is the quantitative dependence between the bonding and thermal conductance. To address this issue we model the heat flow between vertical CNT and Si substrate using molecular dynamics (MD) simulations to systematically study the effect of chemical bonding. We demonstrate that with good covalent bonding, thermal conductance between CNT and Si is almost two orders of magnitude larger than that characterizing an interface with just a van der Waals bonding and much larger than observed in experiment. To gain further insight into this dramatic effect we employ wave packet technique to study the transmission of individual phonons across the Si-CNT interface.

II. SIMULATION PROCEDURE AND MODEL SETUP

Our model system consists of an open-ended (10, 10) CNT adhering vertically to (001) Si surface (see the top panel of Fig. 1). The structure is contained within a rectangular simulation box with a cross section of $43.44 \times 43.44\text{ \AA}^2$ (8×8 unit cells of Si). The Si crystal is composed of 2176 atoms and CNT contains 2000 carbon atoms. Periodic boundary conditions are used in all directions, thus resulting in two Si-CNT interfaces normal to the z direction.

^{a)}Authors to whom correspondence should be addressed. Electronic addresses: hum2@rpi.edu and keblip@rpi.edu.

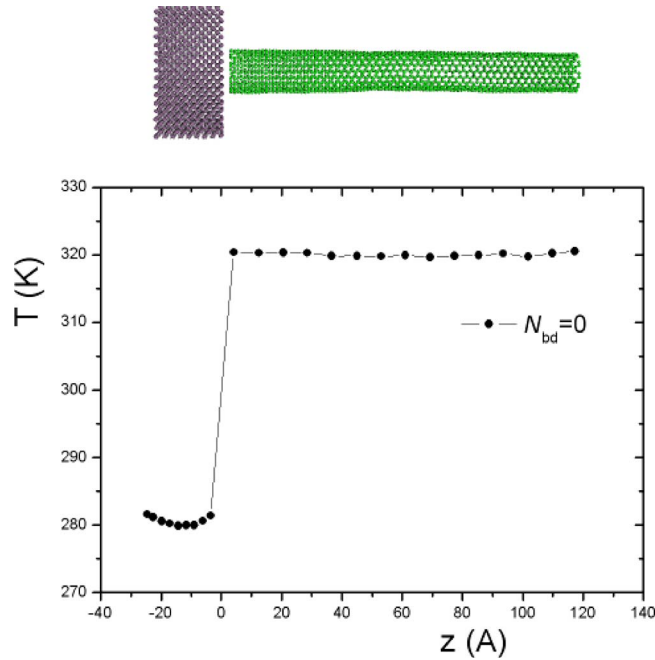


FIG. 1. (Color online) Top panel: snapshot of the whole structure without C–Si covalent bonds. Bottom panel: a typical steady state temperature profile.

The interatomic interactions are described by the polymer consistent force field (PCFF),¹⁴ which include both bonded and nonbonded interactions. In the baseline case the Si and CNT atoms interact just by the nonbonded interactions, which are described by 6-9 Lennard-Jones potential in the PCFF force field. In other structures we introduce covalent bonds between Si and C atoms at the interface and we vary the number of bonds from 1 to 12 per interface.

In the first stage of simulations we equilibrated the system at constant atmospheric pressure and $T=300$ K for 1 ns using integration time step of 0.5 fs. Following equilibration, we fixed the system volume and applied a constant rate heat source in the center of the CNT and removed the heat at the same rate in the center of the Si slab. The heat source and sink were realized using a variant of the algorithm proposed by Jund and Jullien,¹⁵ which conserved the total momentum of the system. To obtain temperature profiles, we divide the simulation box into slices along the z direction, i.e., along the heat current direction. We average the temperature profiles over 100 ps and obtain a series of about 20 temperature profiles for the whole production runs of typically 2 ns. After 500 to 1000 ps (depending on the bond number introduced at the interface) we observe that the temperature profile does not change systematically. The actual reported data represent the steady state averages over the last 1 ns of each production run.

III. RESULTS AND DISCUSSION

A. Effect of chemical bonding on thermal conductance by MD simulation

In the bottom panel of Fig. 1 we show a typical steady-state temperature profile for van der Waals bonded interface, i.e., without covalent bonds ($N_{bd}=0$). Here we define N_{bd} as

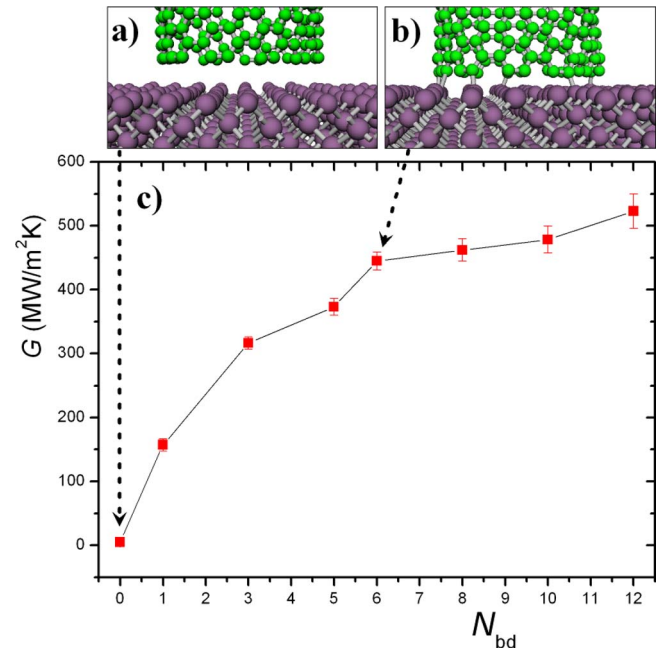


FIG. 2. (Color online) Top panel: snapshots of two interface structures: (a) without C–Si bonds, (b) with six C–Si bonds per interface, and (c) Si–CNT interfacial thermal conductance as a function of C–Si bond number.

the number of C–Si bonds per interface. As clearly seen in Fig. 1, the temperature profile in CNT is flat and has a small but visible slope in Si region. This is due to the low interfacial thermal conductance and large bulk conduction of either silicon or CNT. Therefore the overall temperature drop in the system is dominated by the interface.

The temperature drop ΔT at the Si–CNT interface can be quantified by the relationship¹⁶

$$J_Q = \Delta T / R_K, \quad (1)$$

where R_K defines the interfacial thermal resistance, also known as the Kapitza resistance, and J_Q is the heat flux across the interface. From the data of the temperature drop, according to Eq. (1), we can calculate the interfacial resistance R_K , or equivalently, interfacial conductance $G=1/R_K$. However, the flux requires the determination of the interfacial area. For this purpose we adopted the method of a ring of van der Waals thickness of 3.4 Å.^{17,18} With this definition for the case with only physical interactions present, we obtained the interfacial conductance $G=5.0$ MW/m² K. If we assume that only about 20% of the interface is covered with nanotubes, the corresponding conductance would be about 1 MW/m² K, which is the same as the experimental value for CNT array grown on Si substrate.^{8,10} This agreement can be accidental since in experiment not all tubes (or tube walls) are in actual contact, and some can be in chemical contact.

The dependence of thermal conductance on the number of C–Si bonds is demonstrated in Fig. 2. Here we increase the number of C–Si bonds from 0 to 12. As expected, as the number of bonds increases the interfacial conductance increases. Quite remarkably, a presence of a single covalent bond increases the conductance over one order of magnitude to about 150 MW/m² K. With large number of bonds the

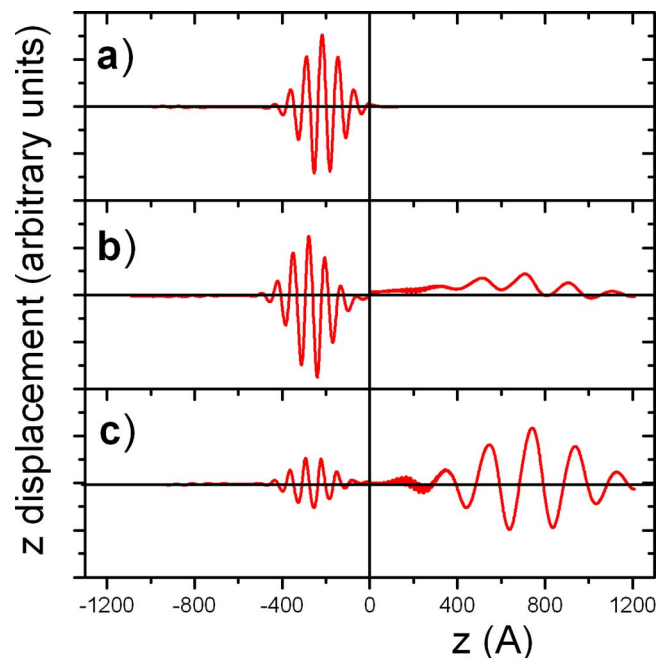


FIG. 3. (Color online) Snapshots of displacements for an LA wave packet with $f=1.10$ THz: (a) before scattering, (b) after scattering: no covalent bonds, and (c) after scattering: with covalent bonds ($N_{bd}=6$).

conductance reaches as high as $500 \text{ MW/m}^2 \text{ K}$, which is two orders of magnitude enhancement compared with that characterizing physically bonded CNT.

Assuming 20% tube coverage the corresponding interfacial conductance would be $100 \text{ MW/m}^2 \text{ K}$. This number is two orders of magnitude larger than measured in experiment.^{8,10} This suggests that there is a significant room for improvement even if partially realized interfacial thermal materials with CNTs covalently bonded to the substrate might be very efficient.

B. Analysis of individual phonon scattering by wave packet technique

To understand the mechanism behind the dramatic effect of bonding on thermal conductance, we performed phonon wave packet dynamic simulations.¹⁹ In this case the simulation cell consists of $3 \times 3 \times 201$ Si slab, which is about 110 nm long in the z direction and 120 nm long (10, 10) CNT. Such lengths are sufficient to study phonon transmission across the interface (located at $z=0$) without interference from boundary scattering.

In the wave packet simulations the whole structure is first relaxed to zero temperature minimum energy configuration. Then a phonon wave packet with well-defined wave vector and polarization is introduced in the silicon slab and starts to propagate toward the interface [Fig. 3(a)]. After arriving at the interface a part of the energy is transmitted and the other reflected [Figs. 3(b) and 3(c)]. The analysis of those energies allows to calculate the transmission coefficient (TC) defined as the ratio of the transmitted to the initial energy.

Figure 3 shows a series of snapshots of atomic displacements for longitudinal acoustic (LA) wave packet with average frequency $f=1.10$ THz. For the case without covalent bonds most of the mode energy is reflected from the interface

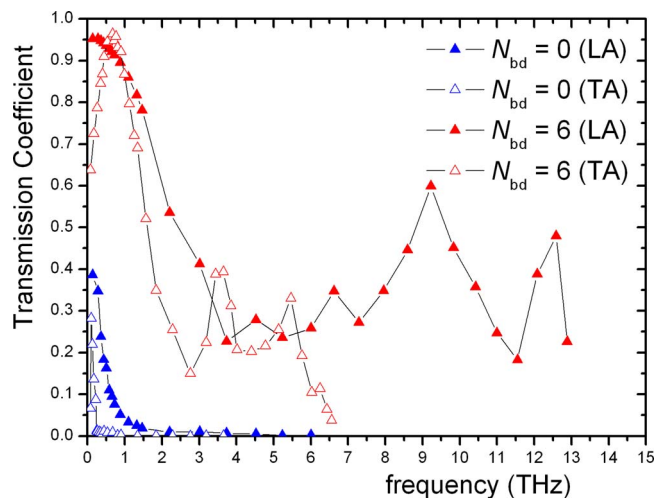


FIG. 4. (Color online) Frequency dependence of the energy TC.

[see Fig. 3(b)], while for the case with covalent bonds most of LA mode is transmitted into CNT and propagates with a higher group velocity but with the same frequency.

Figure 4 shows the frequency-dependent energy TCs for incident LA and transverse acoustic (TA) wave packets. With $N_{bd}=0$ the TC is only appreciable at low frequencies. Furthermore, TCs for LA modes are larger than that for TA modes across the whole frequency range. This is likely associated with the fact that atomic displacements for LA modes are normal to the interface, while displacements for TA modes are parallel to the interface.

With covalent bonds both LA and TA modes have much higher TCs. In particular in the low frequency region the transmission is close to unity, while in the intermediate and high frequency region the coefficients are within 0.2–0.5 range. The intermediate frequency modes are most important for thermal transport as they are more abundant than low frequency modes and have large group velocities. The high frequency modes have very small group velocities and thus are not significant thermal energy carriers. Therefore we conclude that the large difference between thermal conductance of the CNT-Si interface with and without covalent bonds is mainly due to large increase in TCs of intermediate frequency modes due to the presence of covalent bonds. We also note that at room temperature in Si as well as in CNTs, the high frequency modes are not excited since they obey Bose–Einstein distribution.

C. One-dimensional (1D) chain model

In order to understand more quantitatively the origin of frequency and bonding dependence of the TC for LA modes, we consider a simple 1D chain model of masses connected by linear springs. In one semi-infinite half of the chain, the mass, spring length, and spring constant were adjusted so as to reproduce the LA branch dispersion as well as acoustic impedance for Si. Analogously, in the other half, the chain represents CNT properties. The bond between Si and CNT is treated as an adjustable parameter.

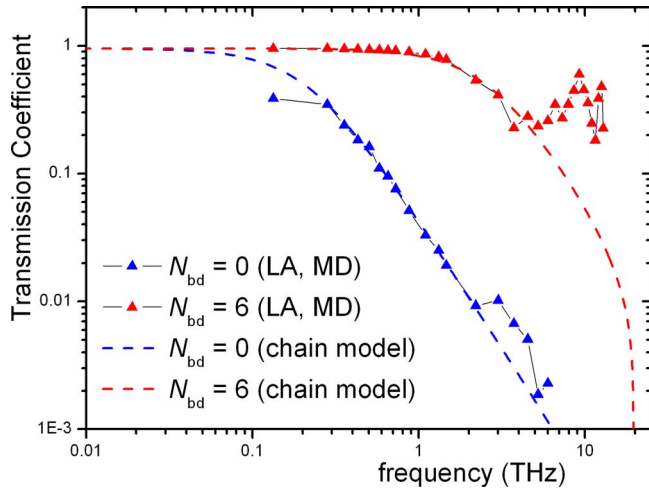


FIG. 5. (Color online) Frequency-dependent energy TC fitted by a 1D chain model.

We calculated the TC as a function of frequency using Green's function formalism and Caroli formula.²⁰⁻²³ For this simple model the following analytical solution of TCs yields

$$\alpha(\omega) = 4k_{\text{Si-CNT}}^2 k_{\text{Si-Si}} k_{\text{CNT}} \sin(q) \sin(q') / |d|^2, \quad (2)$$

where $k_{\text{Si-Si}}$, k_{CNT} , and $k_{\text{Si-CNT}}$ are the stiffness of the springs connecting Si-Si, CNT-CNT, and Si-CNT masses, respectively,

$d = [\omega^2 - k_{\text{Si-CNT}} + k_{\text{Si-Si}}(e^{iq} - 1)][\omega^2 - k_{\text{Si-CNT}} + k_{\text{CNT-CNT}}(e^{iq'} - 1)]$ is the determinant of Green's function of the 1D chain model, and q and q' are the wave numbers of Si and CNT chains, respectively. Then we adjusted the value of the spring constant that connects Si and CNT chains to best fit the data obtained by phonon scattering MD simulations. The results of such fits for $N_{\text{bd}}=0$ and $N_{\text{bd}}=6$ are shown in Fig. 5. The best fit for $N_{\text{bd}}=0$ was obtained with $k_{\text{Si-CNT}}/k_{\text{Si-Si}}=0.013$. Such low value of $k_{\text{Si-CNT}}/k_{\text{Si-Si}}$ is consistent with the fact that there are no covalent bonds between Si and CNT. We also note that the fit for $N_{\text{bd}}=0$ is quite good across the whole frequency range indicating that the mechanism of LA phonon scattering between CNT and Si bonded by physical interactions is well described by the chain model.

The best fit for $N_{\text{bd}}=6$ was obtained with $k_{\text{Si-CNT}}/k_{\text{Si-Si}}=0.15$, which is consistent with the fact that a number of covalent bonds exist between CNT and Si in this case. The fit follows the data very well until the frequency of about 4 THz. For larger frequencies the actual TCs remain in the 0.2–0.5 range (see Fig. 4) while the transmission for the chain model decreases rapidly with frequency. The analysis of the scattering process of high frequency phonons reveals that the incident LA phonon scatters into multiple phonon branches present in CNT. By contrast in the chain model,

there is only one phonon branch. This is likely the reason why the chain model underestimates the transmission of high frequency phonons.

IV. CONCLUSION

In summary, using MD simulations and an analysis of individual phonon scattering and a simple chain model, we demonstrated a dramatic effect of chemical bonding on thermal transport across CNT-Si interfaces. Without chemical bonds between CNT and Si the thermal resistance is high and its values are consistent with that measured in experiment on vertical CNT arrays. With chemical bonds the thermal resistance is reduced by two orders of magnitude. Our results show significant potential of CNT arrays for thermal management well beyond that demonstrated to date by experiment.

ACKNOWLEDGMENTS

This work was supported by the gift from the Intel Corporation and by the New York State Interconnect Focus Center at RPI.

¹Emerging Research Devices, International Technology Roadmap for Semiconductors, 2004 (http://www.itrs.net/Links/2004Update/2004_05_ERD.pdf).

²R. S. Prasher, J. Y. Chang, I. Sauciu, S. Narasimhan, D. Chau, G. Chrysler, A. Myers, S. Prstic, and C. Hu, *Intel Technol. J.* **9**, 285 (2005).

³R. C. Chu, Proceedings of the Rohsenow Symposium on Future Trends in Heat Transfer, Cambridge, MA, 16 May 2003 (unpublished).

⁴C. Yu, L. Shi, Z. Yao, D. Li, and A. Majumdar, *Nano Lett.* **5**, 1842 (2005).

⁵P. Kim, L. Shi, A. Majumdar, and P. L. McEuen, *Phys. Rev. Lett.* **87**, 215502 (2001).

⁶J. Xu and T. S. Fisher, Proceedings of the Intersociety Conference on Thermomechanical Phenomena Electronic System (ITherm '04), 2004 (unpublished), Vol. 1, p. 549.

⁷J. Xu and T. S. Fisher, *Int. J. Heat Mass Transfer* **49**, 1658 (2006).

⁸T. Tong, Y. Zhao, L. Delzeit, A. Kashani, M. Meyyappan, and A. Majumdar, *IEEE Trans. Compon. Packag. Technol.* **30**, 92 (2007).

⁹B. A. Cola, X. F. Xu, and T. S. Fisher, *Appl. Phys. Lett.* **90**, 093513 (2007).

¹⁰B. A. Cola, J. Xu, C. R. Cheng, X. F. Xu, T. S. Fisher, and H. P. Hu, *J. Appl. Phys.* **101**, 054313 (2007).

¹¹S. Shaikh, K. Lafdi, and E. Silverman, *Carbon* **45**, 695 (2007).

¹²C. H. Liu and S. S. Fan, *Appl. Phys. Lett.* **86**, 123106 (2005).

¹³J. K. Diao, D. Srivastava, and M. Menon, *J. Chem. Phys.* **128**, 164708 (2008).

¹⁴H. Sun, S. J. Mumby, J. R. Maple, and A. T. Hagler, *J. Am. Chem. Soc.* **116**, 2978 (1994).

¹⁵P. Jund and R. Jullien, *Phys. Rev. B* **59**, 13707 (1999).

¹⁶E. T. Swartz and R. O. Pohl, *Rev. Mod. Phys.* **61**, 605 (1989).

¹⁷S. Berber, Y. K. Kwon, and D. Tomanek, *Phys. Rev. Lett.* **84**, 4613 (2000).

¹⁸S. Maruyama, *Microscale Thermophys. Eng.* **7**, 41 (2003).

¹⁹P. K. Schelling, S. R. Phillpot, and P. Keblinski, *Appl. Phys. Lett.* **80**, 2484 (2002).

²⁰C. Caroli, R. Combescot, P. Nozieres, and D. Saint-James, *J. Phys. C* **4**, 916 (1971).

²¹J. S. Wang, J. Wang, and N. Zeng, *Phys. Rev. B* **74**, 033408 (2006).

²²J. S. Wang, N. Zeng, J. Wang, and C. K. Gan, *Phys. Rev. E* **75**, 061128 (2007).

²³J. S. Wang, J. Wang, and J. T. Lü, *Eur. Phys. J. B* **62**, 381 (2008).